Thermal Analysis of Power Module Packaging Using Power-System-in-Inductor (PSI^2) Technology

Andrew Yurek, Wenbo Liu, Yan-Fei Liu, *Fellow*, *IEEE*
Department of Electrical and Computer Engineering
Queen's University, Kingston, Canada
13aty@queensu.ca, liu.wenbo@queensu.ca, yanfei.liu@queensu.ca

***Abstract*— This paper presents a thermal analysis of the power-system-in-inductor (PSI^2) packaging for power modules. PSI^2 uses magnetic material as both the power module packaging and magnetic inductor core to increase inductor winding size and thermal conductivity of the package. Two identical buck power modules are designed using the new PSI^2 package and traditional plastic packaging. A thermal equivalent circuit (TEC) model is developed to estimate case and junction temperatures based on estimated loss data. FEA simulation is used to validate the TEC and predict the experimental results. Experimentation is conducted at constant load and loss to compare thermal performance of PSI^2 to conventional plastic epoxy packaging using identical buck power modules. In experimental testing, constant loss experimentation reveals an 8.6 ℃ surface temperature decrease for the PSI^2 package. Therefore, approximately 33% of the PSI^2 temperature decrease is attributed to improved package thermal performance.**

Keywords*— *PSI^2; Thermal equivalent circuit; FEA simulation; low loss

I. INTRODUCTION

Point of load (POL) converters are used today in spatially and thermally constrained applications due to their high-power density and versatile design. Many devices require a range of voltages from the main power supply that are provided by POL converters. The primary challenge in designing these converters is removing heat from the device package to ambient. Heat is generated in POL converters through DC and AC losses. DC losses are primarily attributed to conduction loss of power components. AC losses are primarily attributed switching losses in MOSFETs and magnetic components. These losses become more dominant as switching frequency increases in pursuit of reducing magnetic device size. The loss must be reduced to minimize module size, lower component cost, and decrease the required thermal dissipation. The remaining heat generated by the loss must be dissipated through the POL package to avoid damaging the device.

Research has focused on methods of improving heat transfer from small POL packages [1]. Such methods include passive component integration into PCB substrates [2] [3] [4], and improving module packaging methods [5] [6] [7] [8] [9] To design such packages, research has focused on different thermal modelling and analysis methods to predict the performance of module packages. Such methods focus on accurately estimating loss values [10] [11], or simulating device performance through analytical or FEA methods [12] [13] [14] [15] [16] [17].

Recent research has focused on a packaging method called Power-System-in-Inductor (PSI^2) which integrates a POL power module into the core of the modules inductor [5] [8] [9]. This package is designed to improve the loss and thermal challenges faced by POL converters. Under PSI^2 design, the plastic packaging that traditionally packages the power module is replaced with the magnetic inductor core. This approach allows for the core and winding of the power inductor to increase, which reduces winding resistance, while simultaneously improving the thermal conductivity of the package casing. Thus, heat generation is reduced while heat transfer is improved. Additionally, PSI^2 maintains package size compared to its plastic counterpart.

The objective of this paper is to isolate the thermal performance benefits of the PSI^2 package through analysis, simulation, and experimentation with identical buck power modules using PSI^2 and traditional plastic packages operating in constant loss conditions. Both power modules are tested with identical PCBs, components, and testing environments for accurate results.

This paper is organized into the following three sections: Section II describes the design of the power modules, Section III presents the analytical and simulated thermal results using thermal equivalent circuit (TEC) models and FEA analysis, Section IV presents the experimental thermal results, and Section V concludes the findings of this paper.

II. POWER MODULE DESIGN

Power module packaging typically consists of fixed components encapsulated in plastic epoxy packaging to provide uniform heatsinking and durability. Fig. 1 (a) shows the PSI^2 module with the inductor core semi-transparent. Fig. 1 (b) shows the plastic module with the plastic package semi-transparent. The new PSI^2 packaging method replaces the traditional plastic packaging with the magnetic inductor core. The remaining components of the power module are contained within the cavity of the PSI^2 package magnetic core opposite the inductor winding. To thermally connect the components to the core cavity, thermal paste is applied with the same conductivity as the plastic package.

978-1-7281-1842-0/19/$31.00

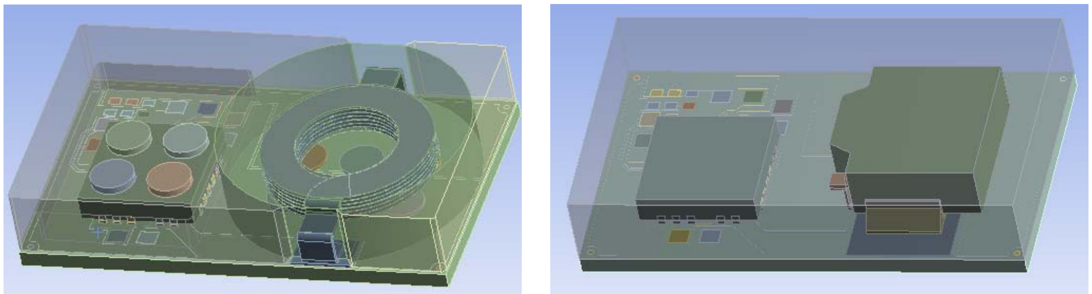

(a) Structure of PSI^2 module (b) Structure of plastic module

Fig. 1. PCB structure of power modules with cases removed.

Synchronous buck power modules with constant on-time are used for testing the packaging design. Additional module components consist of two synchronous MOSFETs, an inductor, and passive components. The fixed inductor of the plastic package is selected based on the parameters defined by the PSI^2 inductor. The same size restrictions are made for both packages. The dimensions of the PSI^2 package are defined as 15x9x3mm. The plastic package must use a fixed inductor with a 2mm maximum height to achieve the same package volume after epoxy coating is complete. The electrical parameters of the fixed inductor are also selected to be the same as the PSI^2 inductor. The maximum current saturation rating is selected at 9.6A. The inductance for both packages is selected at 1uH. The selected fixed inductor has 17.2 mΩ DCR and meets the spatial constraints defined by the PSI^2 package. Table 1 shows the testing parameters for simulation and experimentation.

Table 1: Device specifications for the tested POL converters.

Topology	**Input (V)**	**Output (V)**	**Full Load (A)**	**T$_{\text{ambient}}$ (˚C)**
Buck Converter	12, 24	1.5	8	22

The fabricated PCB's of both packages are identical, except for larger inductor footprints of the plastic package on the top side to accommodate the fixed inductor. Power planes contain thermal vias to transfer heat to the bottom side of the board more effectively. The PSI^2 inductor is soldered on last to encapsulate the components. Fig. 2 (a) shows the fabricated power modules PCBs. This highlights the increased inductor footprint size of the plastic package. Fig. 2 (b) shows the populated plastic power module with the plastic cover removed.

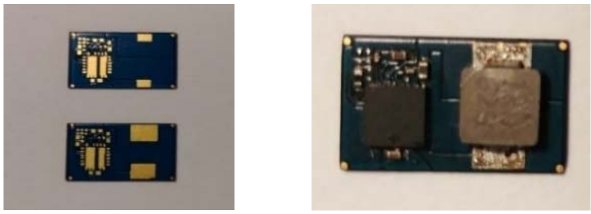

(a) PSI^2 (top) and Plastic (bottom) (b) Plastic, populated

Fig. 2. Fabricated power modules for PSI^2 and plastic packages.

Testing boards are used to mount both modules. These boards provide an interface for the modules to accomodate larger passive components such as large capacitors and lower tolerance resistors. Additionally, the mounting board acts as a heatsink for the bottom side surface of the power modules. Once the modules are mounted to the testing board, the epoxy is poured onto the plastic package using a small plastic mold to encapsulate the plastic module.

III. THERMAL EQUIVLAENT CIRCUIT AND FEA ANALYSIS

In this section, the two packaging types are modelled using an analytical thermal equivalent circuit (TEC) model followed by FEA thermal simulation. The power loss of the modules must be calculated to model the thermal performance of each package. To ensure fair results, the loss of both converters is fixed at 3W. The distribution of loss is not equal for both packages, however, as the winding losses and operating frequency are not equal for both converters at the same total loss. For the buck power modules, the primary loss generating components are the core loss, winding loss, and IC loss. ANSYS Maxwell electromagnetic simulation is used to calculate core loss. The inductance, turns, core area, and the waveform of the winding current are required to simulate core loss. The waveforms of the B field and core loss of the inductor are obtained using electromagnetic simulation. The winding current is obtained by applying the inductor voltage waveform to the winding input terminals. The core loss character, P_v, is calculated using the Steinmetz equation shown below.

$$P_v = C_m B_{pk}^x f^y \tag{1}$$

The Steinmetz coefficients are estimated from the core material. The final core loss for the given inductor volume is calculated using equation (2). The calculated core loss for both packages is shown in Table 3. Since core loss is relatively small and close to the same for both packages, the core loss used is the same for both inductors.

$$P_{core} = P_v A L_e \tag{2}$$

The winding loss is an additional primary loss generator. Winding loss is a conduction loss calculated using equation (3).

$$P_{winding} = I_{out}^2 R_{winding} \tag{3}$$

The output current is obtained experimentally for each package to achieve 3W loss for each package. The winding resistance (DCR) is defined for each inductor. The DCR for the PSI^2 package is 12mΩ. The DCR of the plastic package fixed inductor is 17mΩ. Skin effect is an AC factor that effects winding resistance. Temperature also effects winding resistance.

The DCR is measured at full load switching frequency to estimate real resistance. The PSI^2 resistance is measured at 15mΩ and plastic is 21mΩ under these conditions. The temperature coefficient is estimated at 1.5 for both inductors. The calculated winding loss of both packages are shown in Table 3 below.

The third primary loss component is the IC loss. The loss generated in the IC is primarily generated by the integrated synchronous MOSFETs in the form of conduction (DC) and switching (AC) loss. The hard switching of the converter results in a stronger dominance of switching loss in the IC. For simplicity, the IC loss is estimated as the remaining from the constant 3W loss less core loss and winding loss.

The final key loss contributor is due to the power modules' IC. The key contributor to thermal generation in the IC is the integrated switching MOSFETs. MOSFET loss consists of switching and conduction loss. Since the power modules operate with hard switching, switching loss is dominant and dependent on operating frequency. The same IC is used in both converters, therefore differences in IC loss only depends on the frequency dependent switching loss. The loss of IC was estimated as the remaining amount of total loss after accounting for core and winding loss. The estimated IC loss of both packages is shown in Table 3 below.

To analytically estimate the thermal performance of PSI^2 and plastic package, a thermal equivalent circuit model is developed. The model is based on previous research studied in [14]. A thermal equivalent circuit model allows for an accurate estimation of desired node temperatures based on input power loss and the thermal resistivities of the module materials. The objective of this model is to determine the junction, coil, top surface, and bottom surface temperatures of the modules to compare to FEA and experimental results. FEA simulation is used to calculate constant thermal resistance values using room temperature data input. Table 2 shows the thermal equivalent circuit parameters determined using FEA simulation.

Table 2: Thermal equivalent circuit model parameters.

Designator	**Equivalent Thermal Resistance**	**Value (K/W)**	
		PSI^2	**Plastic**
R1	Case to ambient	28	30
R2	Internal packaging	12	8
R3	Internal packaging	12	50
R4	IC to packaging	6	6
R5	IC to module PCB	10	10
R6	Coil to packaging	2	6
R7	Coil to module PCB	10	10
R8	Module PCB to mounting PCB	1	1
R9	Mounting PCB to ambient	24	24

The power loss input to the thermal equivalent model consists of the three primary loss sources of the power module: winding loss, inductor core loss, and IC loss. The loss is fixed at 3W for this test which is near full load condition for both devices. The load current is recorded for both PSI^2 and plastic modules to achieve 3W of loss. The power loss data is shown in Table 3 below.

Table 3: Loss data for thermal equivalent circuit model.

Power Loss Parameter	**Equivalent Thermal Resistance**	**Value (W)**	
		PSI^2	**Plastic**
P_{winding}	Inductor winding loss	1.193	1.433
P_{core}	Inductor core loss	0.032	0.032
P_{IC}	IC loss	1.775	1.535
P_{Total}	Total loss	3	3

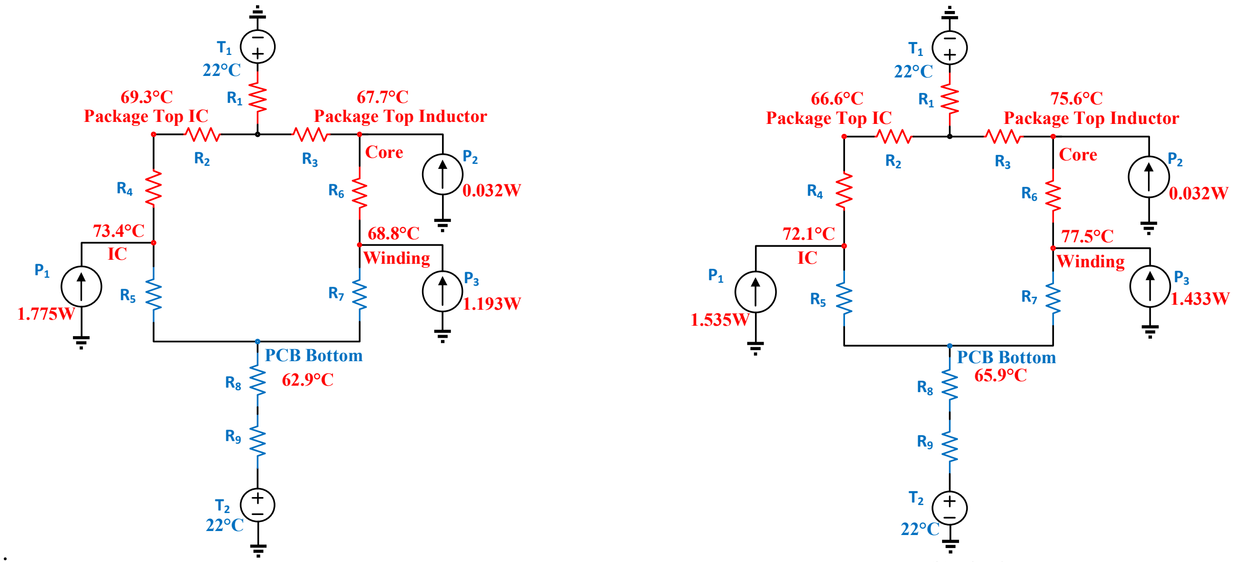

(a) PSI^2

(b) Plastic

Fig. 3. Thermal equivalent circuit models.

The thermal equivalent circuit models are shown in Fig. 3 above. The power loss is input as current sources. The ambient temperatures are applied to the top and bottom surfaces using voltage sources labelled T1 and T2. The analytical results of the thermal equivalent circuit model show a more uniform temperature gradient on the surface of PSI^2 versus plastic packaging with an average temperature decrease of about 7˚C. At the junction level, the IC temperature is nearly the same, while the winding temperature is 8.7˚C cooler for the PSI^2 package. Since the loss of both devices are the same, it is clear the thermal performance of the PSI^2 package is superior to traditional plastic packaging.

Finally, thermal performance of both converters is simulated using FEA through ANSYS software. The inputted losses are shown in Table 3. The loss is applied as heat generation to the inductor core, windings, and the modules' IC. The materials are defined based on the corresponding thermal conductivities listed in Table 4. The thermal conductivity of the PSI^2 package 10x greater than the plastic packaging material.

Table 4. Material thermal conductivity.

Material	**Thermal Conductivity**
PSI^2 Package (MP55 core)	3 W/(m·k)
Plastic Package	0.3 W/(m·k)
Copper	400 W/(m·k)
FR-4 Epoxy	0.3 W/(m·k)
Ferrite	4 W/(m·k)
Silicon	148 W/(m·k)
Solder	48 W/(m·k)

Fig. 4 (a) through (f) show results for an equal 3W loss in both devices. The case and junction temperatures are very similar to the analytically derived temperatures from the thermal equivalent circuit model for both PSI^2 and plastic. A summary of the analytical and FEA simulated temperature results are shown in Table 5 below. The surface temperature of the PSI^2 package is more uniform and cooler than the plastic package due to the improved thermal conductivity of the PSI^2 package. Also, the coil temperature is much lower in PSI^2 due to the improved package thermal conductivity. This additionally results in a slightly higher temperature in the PSI^2 IC as the heat generated in the inductor coil transfers through the case to the IC more effectively. The PSI^2 bottom surface temperature is also slightly higher due to the increase in IC temperature.

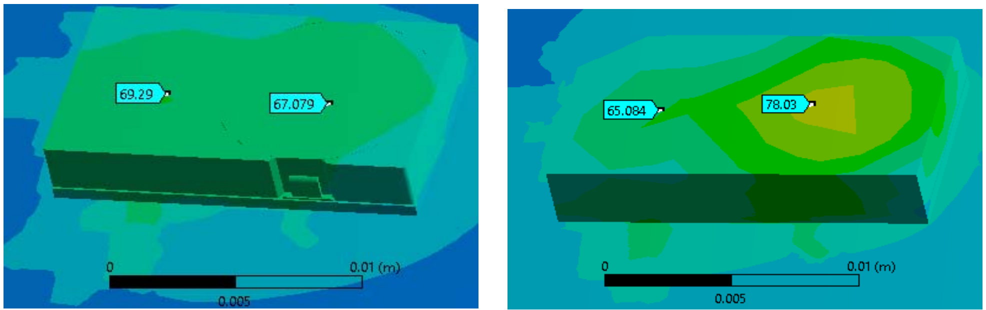

(a) PSI^2 surface (d) Plastic surface

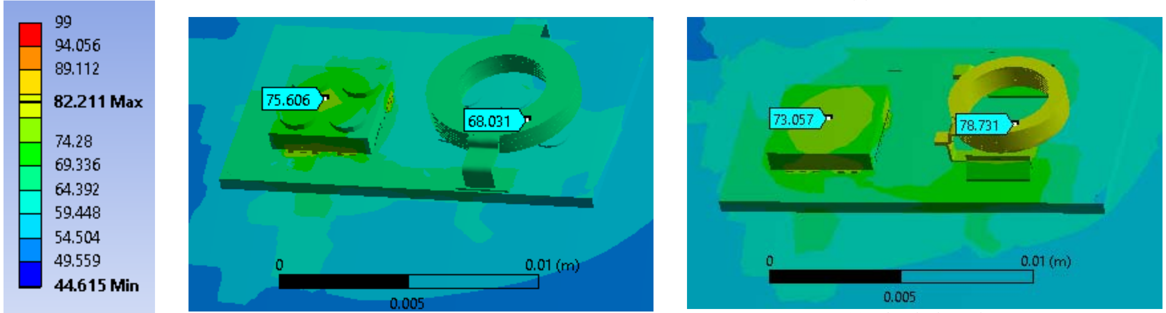

(b) PSI^2 junction (e) Plastic junction

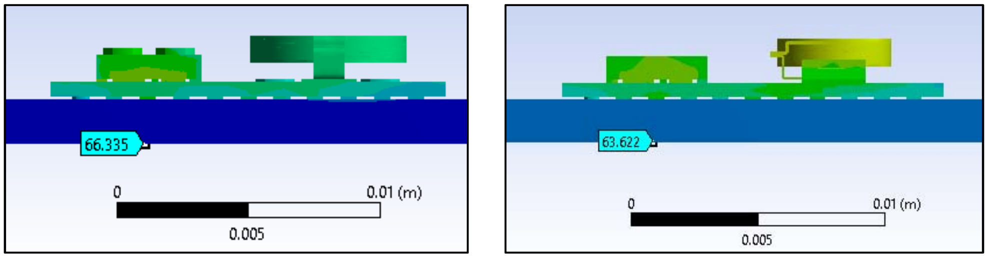

(c) PSI^2 Bottom Surface (f) Plastic Bottom Surface

Fig. 4. Thermal simulation results of surface and junction temperatures at 1.5V, 8A output.

Table 5: Analytical thermal equivalent circuit (TEC) and FEA simulation results.

	PSI^2		**Plastic**	
	Analytical TEC	**FEA Simulation**	**Analytical TEC**	**FEA Simulation**
Package Top IC (˚C)	69.3	69.3	66.6	65.1
Package Top Inductor (˚C)	67.7	67.1	75.6	78
IC Junction (˚C)	73.4	75.6	72.1	73.1
Inductor Winding (˚C)	68.8	68	77.5	78.7
PCB Bottom (˚C)	62.9	66.3	65.9	63.6

IV. EXPERIMENTAL RESULTS

The PSI^2 and plastic modules are experimentally tested to determine the thermal performance of the modules. Testing boards described in Section II are used to mount the modules. The input voltage and load current are varied using DC power supplies and DC loads. The modules are initially tested with a fixed 12V input and 1.5V output to determine the electrical and thermal benefits of PSI^2. Finally, the modules are tested with a fixed loss of 3W at 24V input and 1.5V output to determine the thermal performance of the packages in isolation. The testing board with the PSI^2 module equipped is shown in Fig. 5.

Fig. 5. PSI^2 module mounted to testing board.

The loss of the power modules is measured at varying load currents. Fig. 6 shows the total loss of each module at 12V input and 1.5V output. At full load, the PSI^2 module has approximately 0.5W less loss than plastic module. This is attributed to both the lower DCR of the PSI^2 inductor and lower temperature rise of the PSI^2 package. The PSI^2 package therefore offers better electrical performance compared to the traditional plastic packaging. The PSI^2 package uses package volume more efficiently which allows for larger inductor coil windings and therefore lower DCR.

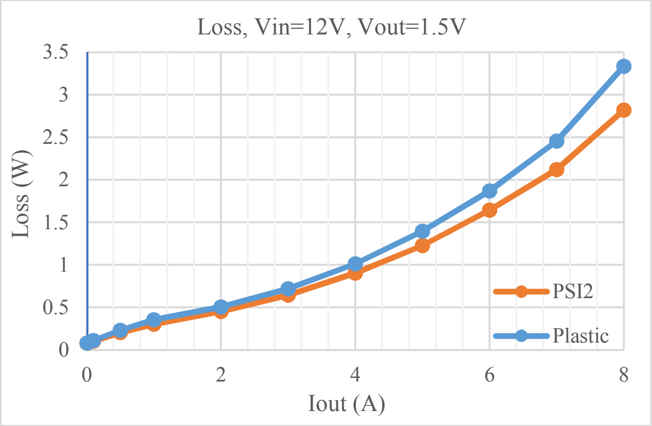

Fig. 6. Comparing loss at different load conditions.

Thermal cameras are used to measure the temperature of the modules and locate any hot spots. Images are captured of the top surface of the module and bottom surface of the testing PCB. To ensure a consistent reading from the thermal camera, the emissivity of the surfaces must be the same. Therefore, a small coating of plastic epoxy is placed on the surface of the PSI^2 module to make sure the emissivity is the same. For this test, the absolute loss difference is being measure which includes the additional loss due to increased winding resistance in the plastic fixed inductor. The load current is increased from 0 to 8A (full load). At full load, the PSI^2 package is 26˚C cooler than the plastic on top, and 5.7˚C cooler on the bottom. This temperature difference is due to both the increased winding loss and poorer package thermal conductivity in the plastic package. Fig. 7 (a) shows the PSI^2 and plastic modules top temperatures versus load current.

Fig. 7 (b) shows the bottom temperatures of the test board for both modules versus load current. Both modules have nearly identical PCB layouts. Component heat generation is being transferred to the bottom of the board primarily through the footprints of the placed components. The largest component footprint for both modules is created by the IC which means it will transfer the most heat to the bottom surface. Both modules use the same IC operating at a similar switching frequency, therefore the bottom temperatures for both modules should be similar.

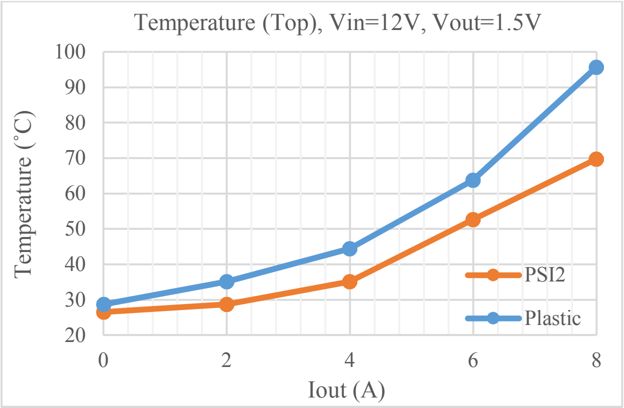

(a) Top temperature vs. load current, 1.5V output.

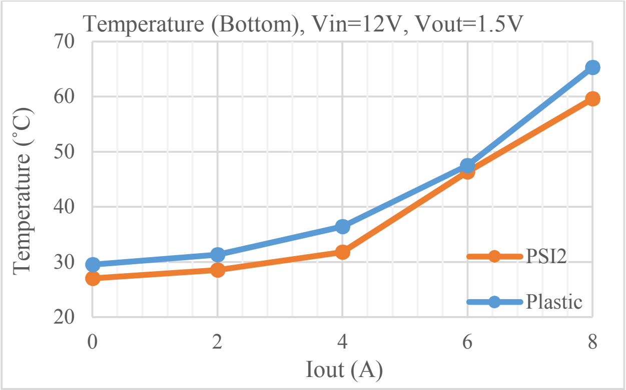

(b) Bottom temperature vs. load current, 1.5V output.

Fig. 7. Comparing bottom temperatures at different load conditions.

A final constant loss test is conducted on both modules. The purpose of this test is to isolate the heatsinking properties from the electrical properties of both packages. The loss of the modules is fixed equally at one, two, and three watts. This testing method removes any temperature disparity due to increased heat generation. Both modules will generate the same total quantity of heat; therefore temperature differences will be the result of the package thermal conductivity. The input and output voltages are the same for both modules. To produce three Watts of loss, the input voltage is set to 24V. The load current is then varied for each module until total recorded loss is 3W. The temperatures are then recorded after some settling time. Fig. 8 (a) shows the top surface temperatures. The PSI^2 top surface package is 8.68˚C cooler on average than the plastic package. Fig. 8 (b) shows the bottom surface temperatures. The PSI^2 package bottom surface is 1.4˚C cooler on average than the plastic package. In the previous constant loss testing. the average top temperature difference at full load was 26˚C, compared to 8.7˚C for constant loss conditions. Therefore, about 17.5˚C of the thermal performance increase between the PSI^2 and plastic package is due to decreased winding loss from lower loss inductor windings. Therefore, the constant loss tests show that the thermal conductivity of the package accounts for approximately 33% of the average temperature difference. Lower loss components and improved thermal conductivity of the PSI^2 package improves overall thermal performance against traditional plastic packaging. The average temperature difference on the bottom surface is very small. Both boards have identical layouts and components except for the inductor therefore this result is expected. The bottom side temperature is also primarily dependent on core and IC loss which are very similar for both packages. This further supports the results.

.

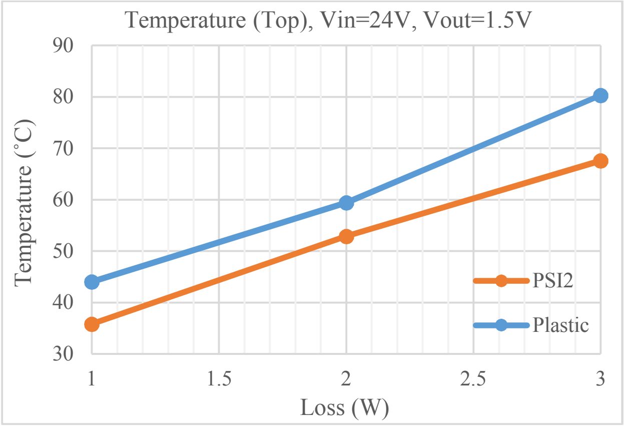

(a) Top temperature vs. loss, 1.5V output.

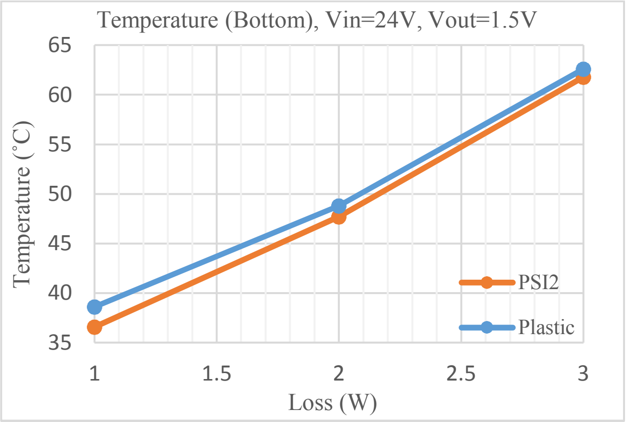

(b) Bottom temperature vs. loss, 1.5V output.

Fig. 8. Bottom temperatures at different loss conditions.

Thermal images are taken to visualize the heat distribution of the power modules. Plastic epoxy is coated on the top sides of both packages so that the thermal camera records the same emissivity for both modules. Thermal camera results are verified by thermocouple measurements. Fig. 9 (a) shows the top surface temperature and (b) shows the bottom surface temperature of the PSI^2 package. Fig. 10 shows the same temperatures for the plastic package. The PSI^2 package is 11°C cooler than the plastic package on the top surface, and 1°C cooler on the bottom surface at 3W loss, 24V input, and 1.5V output. These images confirm the results of the simulated values from Section III and show the superior thermal performance of the PSI^2 package.

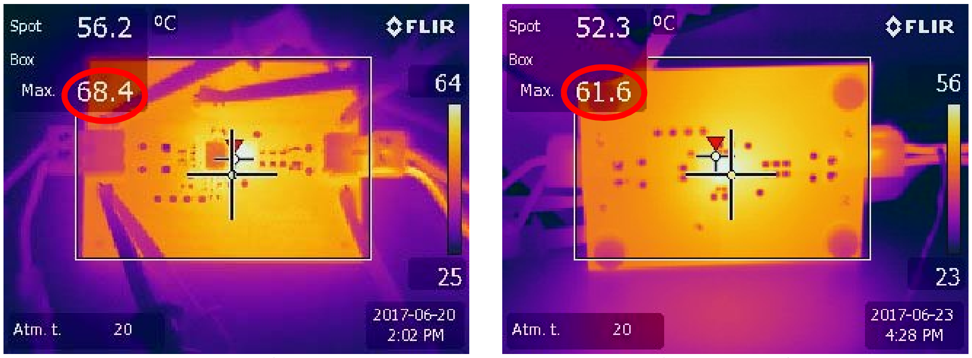

(a) Top Surface (b) Bottom Surface

Fig. 9: Thermal images for PSI^2 packaged module.

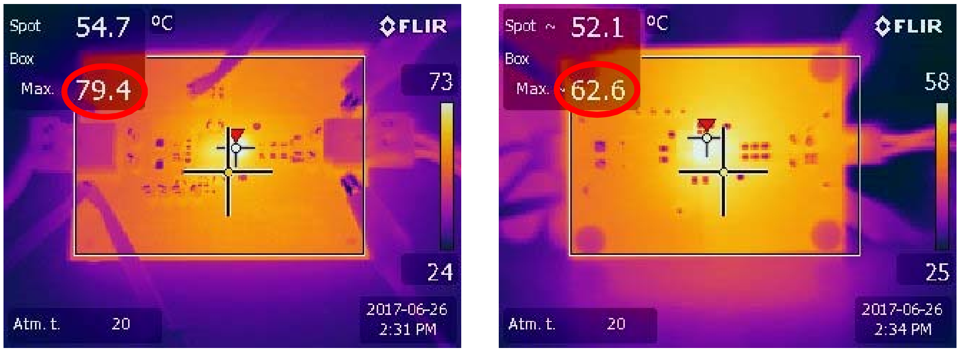

(a) Top Surface (b) Bottom Surface

Fig. 10: Thermal images for plastic packaged module.

A summary of the analytical, simulated, and experimental results is shown in Table 6 below. The results in this table are for 3W total loss, 24V input, and 1.5V output testing conditions.

Table 6: Module temperatures at 3W loss, V_{in}=24V, V_{out}=1.5V

	PSI^2			Plastic		
	Analytical TEC	**FEA Simulation**	**Experimental**	**Analytical TEC**	**FEA Simulation**	**Experimental**
Package Top IC (˚C)	69.3	69.3	68.4	66.6	65.1	-
Package Top Inductor (˚C)	67.7	67.1	-	75.6	78	79.4
IC Junction (˚C)	73.4	75.6	-	72.1	73.1	-
Inductor Winding (˚C)	68.8	68	-	77.5	78.7	-
PCB Bottom (˚C)	62.9	66.3	61.6	65.9	63.6	62.6

V. CONCLUSIONS

This paper analyzes the thermal performance of the PSI^2 package against traditional plastic packaging through an innovative testing combination of analytical and FEA simulation and accurate experimentation with identical buck power modules. The PSI^2 package uses the magnetic inductor core of the power module to replace traditional plastic epoxy as the power module case. Analytical thermal equivalent circuit (TEC) models and FEA thermal simulations are performed on identical power modules to predict the thermal performance of both packages and validate the experimental results. Experimental testing is conducted on power modules with both packaging types under constant load and constant loss testing. The PSI^2 package achieves improved heat transfer, less loss, lower top temperature, and lower bottom temperature compared to the plastic package. Approximately 33% of the measured temperature difference is attributed to the improved thermal heat transfer of the PSI^2 packaging.

REFERENCES

[1] T. Girasek, A. Pietrikova, T. Welker and J. Muller, "Improving thermal resistance of multilayer LTCC module with cooling channels and thermal vias," in *Electronics Technology (ISSE), 2017 40th International Spring Seminar on*, Sofia, Bulgaria, 2017.

[2] P. Artillan, M. Brunet, D. Bourrier, J.-P. Laur, N. Mauran, L. Bary, M. Dilhan, C. Alonso and J.-L. Sanchez, "Integrated LC Filter on Silicon for DC–DC Converter Applications," *IEEE Transactions on Power Electronics,* vol. 26, no. 8, pp. 2319-2325, 2011.

[3] F. C. Lee, D. Reusch and S. Ji, "High-Frequency High Power Density 3-D Integrated Gallium-Nitride-Based Point of Load Module Design,"

IEEE Transactions on Power Electronics, vol. 28, no. 9, pp. 4216-4226, 2013.

[4] J. Sun, D. Giuliano, S. Devarajan, J.-Q. Lu, T. P. Chow and R. J. Gutmann, "Fully Monolithic Cellular Buck Converter Design for 3-D power Delivery," *IEEE Transactions On Very Large Scale Integration (VLSI) Systems,* vol. 17, no. 3, pp. 447-451, 2009.

[5] J. A. Herbsommer, J. Noquil, O. Lopez and J. Sherman, "Integration of power semiconductors devices: Synchronous buck converters in a package," in *Applied Power Electronics Conference and Exposition (APEC)*, Orlando, FL, 2012.

[6] Q. Li, Y. Dong, F. C. Lee and D. J. Gilham, "High-Density Low-Profile Coupled Inductor Design for Integrated Point-of-Load Converters," *IEEE Transactions on Power Electronics,* vol. 28, no. 1, pp. 547-554, 2013.

[7] Q. Li and F. C. Lee, "High Inductance Density Low-Profile Inductor Structure for Integrated Point-of-Load Converter," in *IEEE Applied Power Electronics Conference and Exposition*, Washington, DC, 2009.

[8] L. Wang, D. Malcolm and Y.-F. Liu, "An innovative power module with power-system-in-inductor structure," in *Applied Power Electronics Conference and Exposition*, Long Beach, CA, 2016.

[9] L. Wang, D. Malcolm, Y.-F. Liu and W. Liu, "Thermal Analysis of a Magnetic Packaged Power Module," *Applied Power Electronics Conference and Exposition (APEC), 2012 Twenty-Seventh Annual IEEE,* pp. 2095-2101, 2016.

[10] M. Orabi and A. Shawky, "Proposed Switching Losses Model for Integrated Point-of-Load Synchronous Buck Converters," *IEEE Transactions on Power Electronics,* vol. 30, no. 9, pp. 5136-5150, 2014.

[11] Y.-F. Liu, W. Eberle, Z. Zhang and P. C. Sen, "A simple analytical switching loss model for buck voltage regulators," in *Applied Power Electronics Conference and Exposition*, Austin, TX, 2008.

[12] A. S. Bahman, K. Ma and F. Blaabjerg, "A Novel 3D Thermal Impedance Model for High Power Modules Considering Multi-layer Thermal Coupling and Different Heating/Cooling Conditions," in *Applied Power Electronics Conference*, Charlotte, NC, 2015.

[13] W.-H. Chen, H.-C. Cheng and H.-A. Shen, "An Effective Methodology for Thermal Characterization of Electronic Packaging," *IEEE Transactions on Components and Packaging Technologies,* vol. 26, no. 1, pp. 222-232, 2003.

[14] W. Liu, S. Webb, Y.-F. Liu, L. Wang and D. Malcolm, "A modified equivalent circuit based electro-thermal model for integrated POL power modules," in *Energy Conversion Congress and Exposition (ECCE)*, Cincinnati, OH, 2017.

[15] Z. Luo, H. Ahn and M. A. E. Nokali, "A Thermal Model for Insulated Gate Bipolar Transistor Module," *IEEE Transactions on Power Electronics,* vol. 19, no. 4, pp. 902-907, 2004.

[16] M. Tanaka and Y. Takeuchi, "Thermal Analysis of Plastic QFP with High Thermal Dissipation," in *Electronics Components and Technology Conference*, San Diego, CA, 1992.

[17] B. Trajin, P.-E. Vidal and J. Viven, "Electro-thermal model of an integrated buck converter," in *European Conference on Power Electronics and Applications*, Geneva, Switzerland, 2015.